4-2017

The Impact of a Dynamic Environment on Deposition and Cellular Response to Silver Nanoparticles

Robert F. Uhrig
University of Dayton

The Impact of a Dynamic Environment on Deposition and Cellular Response to Silver Nanoparticles

Honors Thesis

Robert F. Uhrig

Department: Chemical and Materials Engineering

Advisor: Kristen K. Comfort, Ph.D.

April 2017

The Impact of a Dynamic Environment on Deposition and Cellular Response to Silver Nanoparticles

Honors Thesis

Robert F. Uhrig

Department: Chemical and Materials Engineering

Advisor: Kristen K. Comfort, Ph.D.

April 2017

Abstract

Silver nanoparticles (AgNPs) are utilized in many different applications, such as an antibacterial agents or as protective coating against ultraviolet light. However, these AgNPs are known to cause potentially harmful biological effects, including toxicity, induction of stress, and immune activation. In this study, the effects of AgNPs on a human lung cell model were examined within both a static and dynamic environment. Most NP-based research is carried out in static environments, but do not accurate reflect dynamic physiological conditions. Dynamic fluid movement was introduced to the cell culture through the use of a multi-channel peristaltic pump. To further characterize the influence of fluid movement, two different sized AgNPs were tested, 5 nm and 50 nm. The AgNPs were then introduced to the lung cells, under either static or dynamic conditions for a duration of 24-hours. Following this exposure, the cells underwent evaluation for NP deposition, cell viability, cell stress, and inflammatory responses. The results indicated that biological responses were dependent on the delivered NP dosage, which was substantially diminished in a dynamic environment.

Dedication or Acknowledgements

I would like to acknowledge Madison Bourbon for her help with experimentation. I would like to especially acknowledge Dr. Kristen Comfort for all of her support, guidance, and knowledge throughout the thesis process.

UNIVERSITY of DAYTON

Table of Contents

Introduction

In many cases, nanoparticles such as silver can prove to be beneficial. For example, silver nanoparticles (AgNP) are often used for their antibacterial abilities in applications such as dressing wounds and on plastics and apparel. Due to their unique plasmonic and optical properties, AgNPs are also being explored for bioimaging applications. Due to their size, which is smaller than the wavelength of light, AgNPs can enhance both thermal and electrical conductivity, and optically, they can effectively harvest light [1]. Additionally, their ability to reflect light make AgNPs a potential mechanism to protect against UVB radiation [2,3]. For UVB applications, the smaller the primary size, the greater the effectiveness when protecting against the sun [3]. Through these examples, and hundreds of other products and applications, nanoparticles regularly come into contact with human cells, introducing the potential for unintentional consequences. As AgNPs are frequently used for their antibacterial capabilities, exposure occurs primarily through skin contact or inhalation.

While these nanoparticles have benevolent uses, they also are able to induce harmful biological effects; such as toxicity, induction of cellular stress, activation of inflammatory responses, and modification of gene regulation. Once inhaled, AgNPs travel into the lungs and ultimately to the alveoli; which has been shown to be a place of NP accumulation in the body. Additionally, NPs can leave the alveoli and enter into the blood, where they are can accumulate in other areas of the body such as the liver, kidneys, spleen, brain, and heart [4]. In order to best predict the long term implications of NP exposure, scientists have looked closely on how nanoparticles like silver effect the human body within various biological models. NP-induced toxicity and stress levels within the body depend on the unique physicochemical properties of the NP, including composition, surface coating, and primary size [5]. For acute exposures, AgNPs often caused severe damage to the surrounding cells and were found to induce a strong nanotoxicological effect [6]. However, under prolonged low-level exposure, AgNPs were not toxic to cells, but were found to induce high levels of cellular stress and disruption of cellular homeostasis [7].

While studies have examined the effect of nanoparticles on human cells, there have been very few studies that looked at the effect of these nanoparticles in a dynamic environment. However in the limited number of investigations, dynamic flow was found to alter the degree of nanoparticle deposition, nanoparticle behavior, and cellular responses [8], indicating that the recreation of physiologically-relevant fluid dynamics plays a critical role in AgNP-dependent effects. The goal of this project was to further explore the impact of dynamic flow on nanoparticle exposure and subsequent biological responses. This was accomplished by exposing lung cells (A549) to AgNPs within both a static and dynamic environment, in order to characterize differences in deposition and cellular responses. A project summary is shown in Figure 1. This is similar to a study done with AuNPs that developed the dynamic model used in this study [8]; but as AgNPs are known to cause toxicity and stress should illuminate changes to cellular response as a function of flow. The dynamic environment revealed how fluid movement, such as what would be expected in an animal model, would impact deposition and cellular response to various size AgNPs.

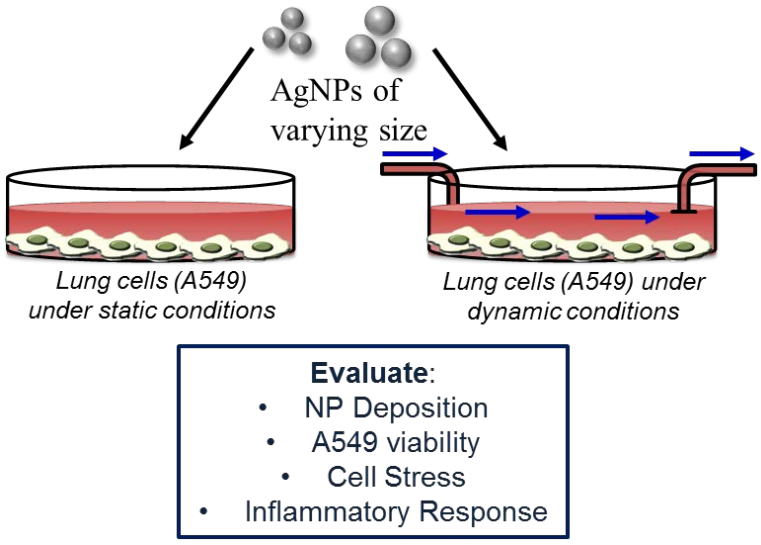

Figure 1: Static and dynamic tests of AgNPs of varying size.

The study dealt with two AgNP sizes, 5 nm and 50 nm. This was done because size has been a predominant factor in AgNP deposition and induced biological response. The surface coating on these AgNPs was polyvinyl (PVP), which was selected owing to the

known stability of PVP-coated NPs. The A549 cells were then exposed to the AgNPs, under either static or dynamic conditions, for a duration of 24 hours. Lung epithelial, A549, cells were selected due to the high rate of inhalation exposure and the strong presence of fluid dynamics in the alveoli. Following the AgNP exposure, the cell responses were evaluated through multiple metrics including cell viability, cell stress, and inflammatory response. These cellular responses were then correlated to the rate of AgNP deposition within the A549 cells.

The first objective was to identify the degree of deposition (fraction of administered dosage that is taken up by the cells) for each experimental AgNP, under both static and dynamic conditions. A549 cells were cultured in RPMI 1640 media supplemented with 10% fetal bovine serum. The cells were then seeded into 24 well plates and exposed to 15 µg/mL of the AgNPs under either static or dynamic conditions. The pump system that was previously established [8], was used in this study. Following a 24-hour exposure, the nanoparticle concentration within the media was determined via UV-VIS analysis. The difference between the final dose and 15 µg/mL was the identified deposited dosage.

The next objective was to expose A549 cells to AgNPs within both the static and dynamic system and examine cellular viability and stress. The cells were exposed to silver nanoparticles of varying size under static or dynamic conditions for 24 hours. The A549s then underwent analysis for both cell viability and cellular stress. The goal of this objective was to determine if and to what degree dynamic flow modified silver nanoparticle induced cellular responses. Cell viability was determined using the MTS assay from Promega, in accordance with the manufacturer's protocol. Cellular stress was measured through quantification of reactive oxygen species (ROS) levels, using the DCFH-DA fluorescence probe from Invitrogen.

The third objective was to examine the inflammatory response to silver nanoparticles through quantification of secreted cytokines IL-6 and TNF-α. Beyond the general toxicity profile induced by silver nanoparticles, this project will explore the A549 inflammatory response to AgNPs. When cells identify a foreign object that they view as a threat, an

inflammatory response is initiated and cytokines are secreted. Therefore, the inflammatory response by the A549 cells was determined following AgNP exposure (25 µg/ml) under static and dynamic conditions. The concentration of target cytokines (IL-6 and TNF-α) secreted into the cell culture media were evaluated using protein-specific ELISAs by ThermoFisher Scientific, in accordance with the manufacturer's instructions.

Following collection of all the data, the static and dynamic conditions were directly compared. Additionally, the A549 responses were correlated to the calculated silver nanoparticle deposition efficiency. Under dynamic flow, silver nanoparticle deposition was significantly reduced. This reduction lead to less induction of cellular toxicity, stress, and inflammatory response. Through implementation of the dynamic exposure system, this project used a system that more accurately resembled the nature of the human body compared to a static environment.

Materials and Methods

Nanoparticle Characterization

Transmission Electron Microscopy (TEM)

TEM was used to analyze the size and morphology of the AgNP stocks. An example TEM image of silver nanoparticles is shown below, in Figure 2.

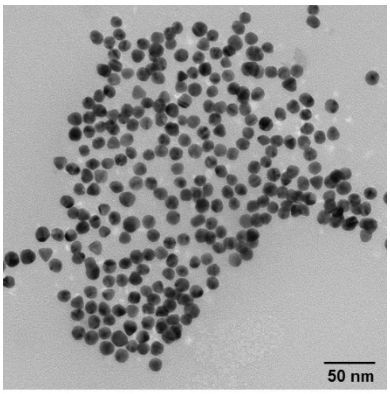

Figure 2: Representative TEM image of 5 nm silver nanoparticles.

1. The AgNP stock solutions were removed from storage at 4°C and vortexed to ensure a homogeneous particle solution.
2. Using a micropipette, one drop of AgNP solution (about 20 μL) was placed onto a TEM grid (Electron Microscopy Sciences) and dried before imaging.
3. The grid, with the AgNPs, was imaged using a Hitachi H-7600 microscope.
4. The spherical morphology of the AgNPs was verified via inspection using the obtained TEM images.
5. The average primary particle size was determined using Image J software. Image J compares pixel numbers to a known size standard, included in the TEM image, to produce particles sizes. For each set of AgNPs approximately 25 NPs were sized to determine average primary size..

Dynamic Light Scattering (DLS)

DLS was used to determine the amount of agglomeration, or clumping, of the AgNPs. DLS works through monitoring the angle of which light deflects following interactions with the NP agglomerates in solution.

1. The AgNP stock solutions were removed from storage and vortexed to ensure a homogeneous solution.
2. The AgNP stock solutions were diluted to 25 μg/mL in either water or cell culture media.
3. The AgNP samples were translocated into an assay cuvette and placed into the analysis chamber of a Malvern Zetasizer Nano ZS.
4. DLS analysis was performed on each sample in triplicate, with pre-programmed settings for silver. The hydrodynamic diameter, which is equivalent to the agglomerate size, was recorded in nm.

Zeta Potential

Zeta Potential was the method used to determine the surface charge of the AgNPs.

1. The AgNP stock solutions were removed from storage and vortexed to ensure a homogeneous solution.
2. The AgNP stock solutions were diluted to 25 μg/mL in either water or cell culture media.
3. The AgNP samples were translocated into an assay cuvette and placed into the analysis chamber of a Malvern Zetasizer Nano ZS.
4. Zeta potential analysis was performed on each sample in triplicate, with pre-programmed settings for silver. The surface charge for each independent trial was recorded in mV.

Ultraviolet–visible spectroscopy (UV-Vis)

UV-Vis was used to determine the absorption spectrum for the experimental AgNPs.

1. The AgNP stock solutions were removed from storage and vortexed to ensure a homogeneous solution.

2. The AgNP stock solutions were diluted to 25 μg/mL in either water or cell culture media.
3. 100 μL samples of the diluted AgNP stocks were placed into individual wells of a 96-well plate.
4. The well plate was inserted into a SpectraMAX Plus 190 microplate reader and the absorbance of the samples were analyzed at wavelengths between 300 and 700 nm, in 10 nm increments.
5. The spectral profiles were observed by plotting the collected absorbance data.

In vitro Responses

Cell Culture

The A549 cells were maintained at proper conditions prior to experimentation. Cell cultures were split approximately every 3-4 days for maintenance.

1. The A549 human alveolar epithelial cell culture was purchased from American Type Cell Culture (ATCC).
2. The cell cultures were grown on tissue culture treated petri dishes (BD Falcon) in RPMI 1640 (Life Technologies) medium supplemented with 1% penicillin/streptomycin (Life Technologies) and 10% fetal bovine serum (Life Technologies). The cells were stored in a humidified incubator maintained at 5% CO_2 and 37°C.
3. The cells cultures were split when the cells were about 90% confluent, as determined via visualization using a light microscope.
4. The media was aspirated off and the culture was washed with 5 mL of phosphate buffered saline (PBS) (Life Technologies).
5. Following the wash, 3 mL of 0.25% trypsin (Life Technologies) was added and the culture was incubated for about 5 minutes until the cells detached from the bottom of the petri dish.
6. Approximately 3 mL of fresh media was added to the cells and they were mixed via pipetting to break up any cell clumps.
7. Approximately 1 mL of the cell mixture was transferred to a new plate and combined with 9 mL of fresh media, swirled to mix, and returned to the incubator.

8. Steps 3-7 were repeated every 3-4 days, as needed, for regular cell maintenance.

Cell Counting/Plating

For experimentation, the A549 cells were counted and plated into the appropriate plate at equal cell densities.

1. A petri dish of A549 cells was removed from the incubator, washed with PBS, and incubated with 3 mL of trypsin.
2. Once the cells were detached from the petri dish, 3 mL of fresh media was added and the cells were mixed to break up large cell clumps.
3. 10 µL of the cell solution was mixed with 10 µL of 0.4% trypan blue stain (Invitrogen) in a single well of a 96-well plate.
4. 10 µL of this mixture was pipetted into one side of a Countess counting chamber slide.
5. The slide was inserted into a Countess Cell Counter (Invitrogen) and the cells sample underwent analysis to determine a live cell concentration. The Countess Cell Counter functions by counting the cells with a stained exterior (dead) and subtracting those from the total amount of detected cells (dead and alive).
6. The remaining cell mixture was diluted to the desired plating concentration with fresh media and plated into 24-well plates for experimentation.
7. The well plate was returned to the incubator overnight to allow the cells time to equilibrate and grow.

AgNP Exposure within the A549 Cultures

Following the overnight incubation of the A549 cells within the 24-well plates, the cells AgNPs were introduced to the A549 at predetermined concentrations and environmental conditions.

1. The AgNP stock solutions were removed from storage and vortexed to ensure a homogeneous solution.
2. The AgNP stock solutions were diluted to either 5 or 25 µg/mL in cell culture media.
3. The media within the 24-well plate were removed and the A549 cells were washed with 500 µL of PBS.

4. For static exposures, the A549s were replenished with either the prepared AgNP solution (750 µL) or fresh media. For dynamic exposure, the A549s were replenished with either the prepared AgNP solution (2.25 mL) or fresh media. The extra volume was added to prime the tubing associated with the peristaltic pump. The well plate was returned to the incubator for 24 hours.

AgNP Deposition within the A549 Cultures

The deposition of the AgNPs, or the percentage of administered AgNPs that were internalized by the cells, was determined under both static and dynamic conditions.

1. A549 cells were plated in a 24-well plate at 7.5 x 10^5 cells/mL, incubated overnight, and underwent the AgNP exposure procedure and outlined above.
2. Following the 24 hour exposure, the media was collected into tubes and stored at -20 °C until deposition analysis.
3. For deposition analysis, 100 µL of media samples were added to a 96-well plate, in triplicate. Additionally, fresh 5 and 25 µg/mL AgNP stock samples were added to the 96 well plate.
4. The plate underwent UV-Vis analysis to determine the spectral profile.
5. Using trapezoidal rule, the area under the spectral curve was calculated, which is directly proportional to AgNP concentration. This data was used to determine the concentration of AgNPs remaining in the media, with the difference between the administered dose and the media concentration equal to the deposited dose.

Lactate Dehydrogenase (LDH) Release

The release of LDH from the A549 cells was used to determine cellular viability following AgNP exposure.

1. A549 cells were plated in a 24-well plate at 7.5 x 10^5 cells/mL and underwent the above exposure steps.
2. At the end of the 24 hour exposure, 75 µL of lysis buffer was added the wells designated as the positive control. This buffer lysed all the cells, providing a LDH level representative of 100% toxicity.

3. For all wells, including the positive control, 100 µL of media was removed and transferred to a 96-well plate.
4. The quantities of LDH in the media was determined using the CytoTox 96 Non-Radioactive Cytotoxicity Assay (Promega), in accordance with the manufacturer's instructions. The steps are outlined below.
5. Following preparation of the assay buffer, 50 µL was added to each well and incubated in the dark at room temperature for 30 minutes.
6. After 30 minutes, 50 µL of Stop solution was added to each well and the absorbance was read at 490 nm using the SpectraMAX Plus 190 microplate reader.
7. LDH release was calculated as a percent of the negative control wells from the same plate via the following equation: $\% \, LDH \; Release = 100 * (\frac{Absorbance_{treated}}{Absorbance_{control}})$.

Reactive Oxygen Species (ROS) Production

Intracellular ROS levels were monitored to determine activation of intracellular stress.

1. A549 cells were plated in a 24-well plate at 7.5 x 10^5 cells/mL and incubated overnight.
2. Dry 2',7'-dichlorodihydrofluorescein diacetate (DCFDA) powder (Invitrogen) was rehydrated in dimethyl sulfoxide (DMSO) (Fisher) to an initial concentration of 1 mM.
3. This DCFDA solution was diluted to a final working concentration of 100 µM in PBS.
4. The cells were washed with PBS, and 500 µl of the diluted DCFDA and PBS mixture was added to each well. The well plate was returned to the incubator for 30 minutes.
5. AgNP exposure solutions were created by diluting vortexed AgNP stock solutions to 0, 5, and 25 µg/ml in cell culture media.
6. After the DCFDA and PBS solution incubation, the cells were washed with PBS, and 750 µl and 2.5 mL of the AgNP exposure solutions were added to each wells for static and dynamic conditions, respectively. The cells were returned to the incubator.

7. After the 24 hour exposure, the ROS levels were determined using fluorescence microscopy on a SpectraMAX Plus 190 microplate reader. The fluorescence settings were an excitation wavelength of 485 nm and an emission wavelength of 538 nm.
8. ROS production was calculated as a percent of negative control from untreated wells on the same plate using the following equation: $\%\ ROS\ production = 100 * (\frac{Fluorescence_{treated}}{Fluorescence_{control}})$.

Enzyme-Linked Immunosorbent Assay (ELISA) Protocol

ELISA tests were used to determine the immune response of the cells based on IL-6 and TNF-α cytokine secretion levels.

1. A549 cells were plated in a 24-well plate at 7.5 x 10^5 cells/mL, incubated overnight, and underwent the AgNP exposure procedure and outlined above.
2. Following the 24 hour exposure, the media was collected into tubes and stored at -20 °C until ELISA analysis.
3. The concentrations of IL-6 and TNF-α within the media samples were determined using protein specific ELISAs (Thermo Fisher Scientific). In addition to the experimental samples, standards of 0, 15.6, 62.5 and 250 pg/mL were analyzed. The use of standards allowed for the creation of a standard curve.
4. The IL-6 and TNF- α ELISAs were carried out in accordance with the specific manufacturer's instructions.
5. At the end of the assays steps, the absorbance of the plate was read at 450 nm using the SpectraMAX Plus 190 microplate reader.

Variations on In vitro Systems

Dynamic Flow Exposure System

The dynamic flow environment was created and used to simulate in vivo conditions, through mimicking fluid dynamics arising from the cardiovascular system. An image of the dynamic system is shown below in Figure 3.

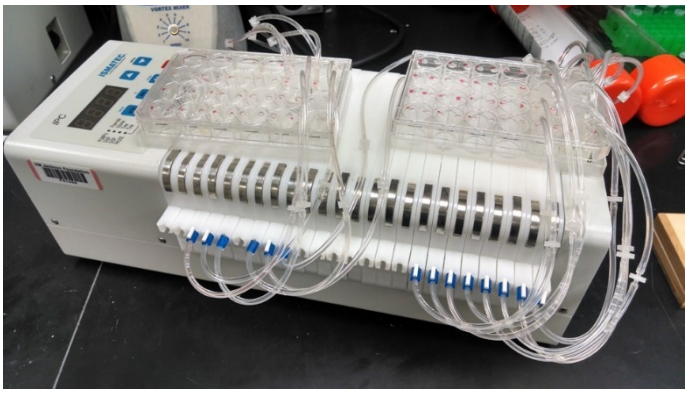

Figure 3: Visualization of the system used to generate a dynamic flow environment.

1. A 24-channel peristaltic pump (Ismatec, model #ISM939D) provided the flow with each channel exclusively connected to a single well of a 24-well plate.
2. 1/16-inch inner diameter tubing from each channel was secured through the lid of the 24-well plate to ensure that the inlet and outlet tubing for each channel remained at opposite ends of each well, providing unidirectional flow.
3. For each experiment, an extra 1.5 mL of media or AgNP solution was added to each well. This extra fluid was there to prime the tubing and to ensure that the liquid height remained the same for both static and dynamic conditions.
4. The pump, tubing, and 24-well plate were stored within the incubator to maintain optimal cell culture conditions of 5% CO_2 and 37°C during experimentation.
5. Calibration was conducted to correlate the pump settings to volumetric flow rates (in mL/min) as follows:
    a. The inlet end of tubing was placed into a reservoir of water and the outlet into a graduated cylinder.
    b. The length of tubing was primed with water from the reservoir to ensure measurement would be immediate and accurate.
    c. A pump setting of interest was selected and the pump was run for 60 seconds.
    d. After the 60 second run, the volume of water in the graduated cylinder was measured and recorded.
    e. This process was repeated for pump settings between 5.90 and 0.2 RPM.
    f. A calibration curve was created with this data for interpolation of any desired pump setting.

6. Volumetric flow rates were converted to linear velocity (cm/s) through the following steps:
    a. The inner diameter tubing of 1.52 mm was utilized to determine the cross-sectional area of the tubing via the equation $A = \pi * r^2$ where A is the cross-sectional area, π = 3.14, and r = inner radius of tubing = 0.076 cm. This yielded a cross sectional area of A = 0.0182 cm^2.
    b. Using the cross-sectional area, each volumetric flow rate (mL/min) was converted to linear velocity (cm/sec) via the equation $Q = V * A$, where V = linear velocity and Q = volumetric flow rate.
7. Once the pump settings were converted to linear velocities, a pump setting was selected 0.89, which correlated to a linear velocity of 0.2 cm/sec, the standard linear velocity for capillaries.

Results and Discussion

AgNP Characterization

Prior to introduction into the cellular system, the AgNPs underwent numerous characterization assessments to quantify the unique physicochemical properties of each NP stock. Representative TEM images of the 5 and 50 nm AgNPs are shown in Figure 4, and demonstrate spherical morphology for both particles. Using multiple TEM images, the primary sizes for the 5 and 50 nm AgNPs were determined to be 5.3 ± 1.4 and 52.6 ± 6.9 nm, respectively. The uniformity of the AgNP stocks was further verified through spectral analysis (Figure 4C). The single, sharp peaks associated with both experimental NPs confirm an equal size distribution and lack of contaminants. Additionally, there is a right-shift associated with the 50 nm AgNPs, which occurs due to the increase in particle size.

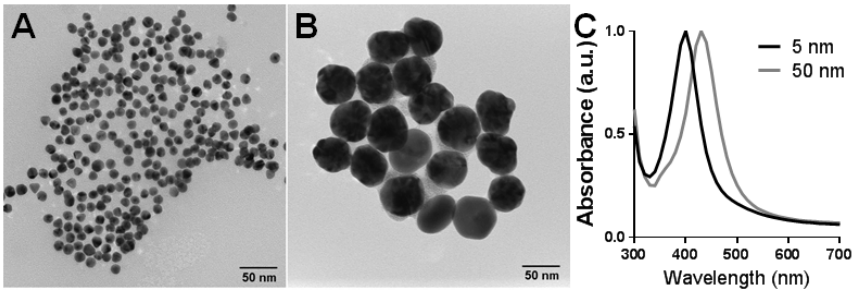

Figure 4: Characterization of AgNP stock solutions. Representative TEM images of the experimental (A) 5 nm and (B) 50 nm PVP-coated AgNPs. The images verify spherical morphology and even particle size distribution. (C) The spectral images for both sets of AgNPs in water demonstrate a sharp, single peak.

In addition to verifying the primary particle size, the agglomerate sizes were determined (Table 1). As all NPs will agglomerate when dispersed in a solution, it is important to assess how extensive the agglomeration is as it can impact mechanisms of biotransport. The AgNPs displayed minimal agglomeration in water with an increased effective diameter size in media, due to the presence of protein in the media. As the NPs had a PVP surface coating, which is known to promote particle stability in solution, the small extent of aggregation was expected. Additionally, the surface charge was assessed using

zeta potential measurements. The stock AgNPs displayed a negative surface charge, approximately -30 mV. Following the formation of a protein corona in media the charge shifted to approximately -10 mV, due to the slightly negative charge of proteins bound to the NP surface.

Table 1: AgNP Characterization

	Size (nm)	**Agglomerate Size (nm)**		**Zeta Potential (mV)**	
		Water	*Media*	*Water*	*Media*
5 nm	5.3 ± 1.4	8.7 ± 0.9	19.3 ± 2.5	-27.7 ± 1.1	-10.6 ± 0.8
50 nm	52.6 ± 6.9	78.6 ± 3.0	89.3 ± 2.2	-30.4 ± 1.7	-9.2 ± 0.6

Generation of a Dynamic Cellular System

To generate a dynamic system, a peristaltic pump was used during experimentation. The pump was an essential part of the experiment because it differentiated the system between static and dynamic. The dynamic environment creates a more physiologically relevant system since the human body is far from static. The pump was operated at a volumetric flow rate which created a linear velocity of 0.2 cm/sec within the tubing. This velocity is equivalent to the velocity within capillaries, meaning that the A549 cells underwent low-level shear stress similar to that experienced within the tissues. This low level shear stress produces a morphological change to A549 cells, which in a dynamic environment display an elongated shape in the directionality of flow (Figure 5).

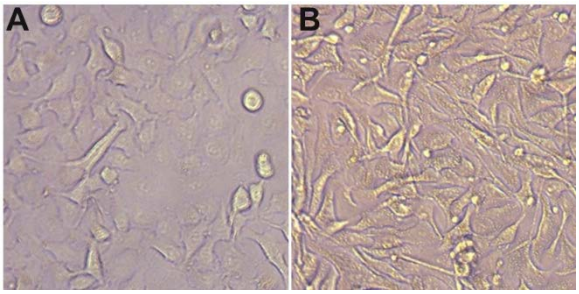

Figure 5: A549 morphology as a function of flow. Representative images are shown for A549 cultures within (A) a static and (B) a dynamic environment. In static incubation, A549s are globular in shape. However, following incubation under dynamic flow, the cells demonstrate elongation.

Dynamic Flow Modifies AgNP Deposition

Next, we investigated how the presence of dynamic flow influenced the degree of AgNP deposition, for both the 5 and 50 nm particle sets. As seen in Figure 6, dynamic flow impacted the AgNP deposition; decreasing the nano-cellular interactions for both particles though not equally. The greatest deposition occurs with the 50 nm in a static environment. As the 50 nm particles have greater mass than the 5 nm set, it makes sense that they would have greater deposition. There is a drop in deposition under dynamic flow, due to the movement the pump creates. Similar results occur with the 5 nm particles, although the static deposition was not as great as the 50 nm set. Within the dynamic environment, there is an even greater drop in deposition, due to the smaller materials being more susceptible to biotransport effects.

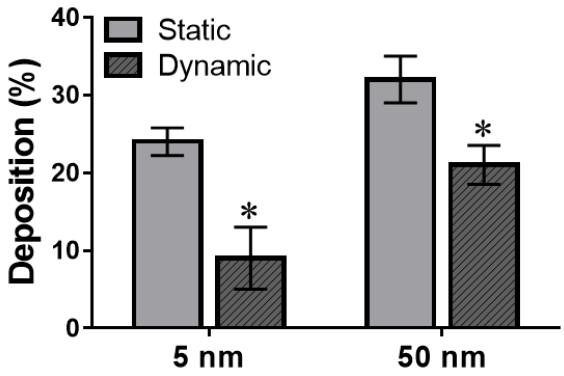

Figure 6: AgNP deposition varies as a function of primary particle size and flow environment. Following a 24 hour incubation, the AgNP deposition within an A549 model was measured for both 5 and 50 nm particles within both a static and dynamic environment. * indicates significance between static and dynamic, n=3, $p<0.05$.

Cellular Responses to AgNPs

Following AgNP exposure, A549 viability was determined by using the LDH test. From this, the cells were evaluated for a range of concentrations (0, 5, and 25 μg/mL). The viability results are shown in Figure 7. Looking first at the 5 nm AgNPs, there was an approximate 30% loss of cell viability after exposure to the high dosage in static conditions. The lower dosage was not associated with any cytotoxicity. Within the dynamic environment, the A549s had a much greater survival rate than within in the

static environment. Looking at the 50 nm AgNPs set, there was a greater cytotoxic response in the static environment, with an approximate 45% toxicity rate. Additionally, while dynamic flow did reduce the cytotoxicity, this response was noticeably less significant than with the 5 nm AgNPs. The collected cell viability is in agreement with deposition in that the dynamic environment yielded less cell death, and the smaller particles were impacted more by the different environments.

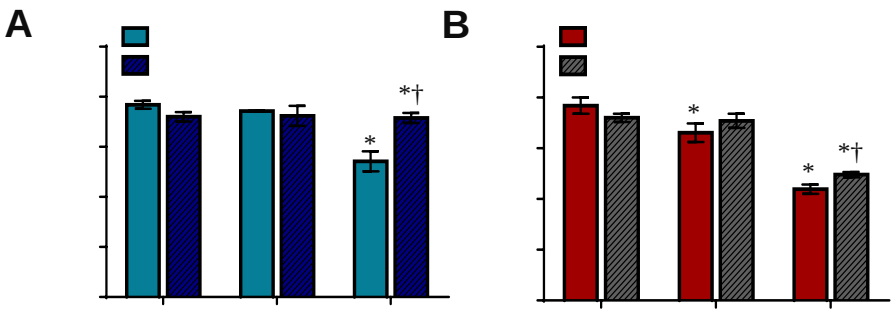

Figure 7: Cellular viability following AgNP exposure. The A549 cells underwent a 24 hour exposure to either (A) 5 nm or (B) 50 nm AgNPs under the stated conditions. For both AgNP sets, A549 viability was a function of both primary particle size and flow environment. * and † indicate statistical significance from untreated control and between static and dynamic conditions, respectively. n=3, $p<0.05$.

Next, detection of ROS levels was used to monitor the cellular stress induced by the AgNPs. As shown in Figure 8, the static 50 nm particles caused the cells the greatest amount of stress, in agreement with the cell viability data. Within a dynamic environment, the amount of cell stress was decreased in both the 5 and 50 nm systems. While 5 nm AgNP exposure did produce intracellular ROS, 5 nm exposure within a dynamic environment demonstrated stress levels equal to the untreated control. This data, which suggests that AgNP-induced stress was diminished under dynamic environments, also strongly aligns with both deposition and viability results.

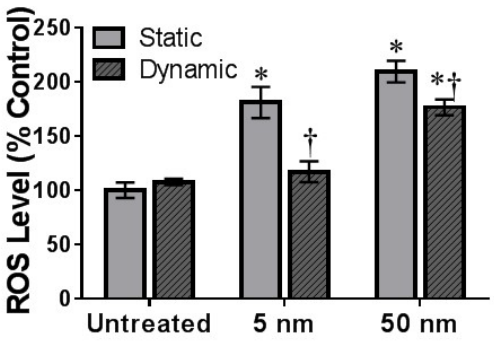

Figure 8: Intracellular ROS levels following AgNP exposure. ROS levels, which are a recognized marker of cellular stress, were determined after a 24 hour exposure under the denoted conditions. ROS levels were a function of both particle size and flow condition, with a significant decrease in ROS associated with fluid flow conditions. * and † indicate statistical significance from untreated control and between static and dynamic conditions, respectively. n=3, $p<0.05$.

Next, the innate inflammatory response of the A549 cells to the AgNPs was determined. Both TNF-α and an IL-6 tests were run to monitor the immune response of the cells. For the TNF-α, there was not a noticeable effect for any of the experimental conditions (Figure 9A). For IL-6 evaluation, 5 nm AgNP exposure induced no change to IL-6 production. However, for the static 50 nm exposure, there was a significant increase in IL-6 production. Under dynamic exposure, the 50 nm AgNPs did not elicit an IL-6 response. This once again shows the impact of a dynamic environment since each dynamic environment gave relatively constant IL-6 secretion. The static 50 nm environment does coincide with previous results since this is the system that the cells had the greatest deposition, toxicity, and stress.

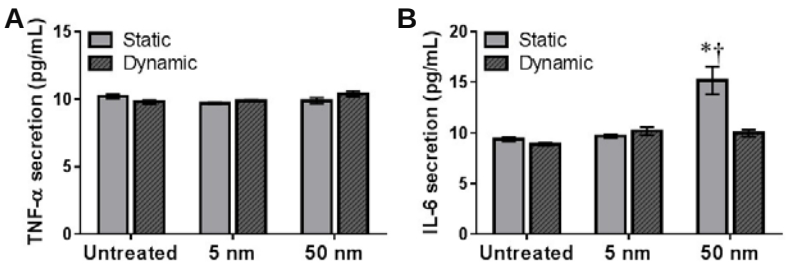

Figure 9: The A549 inflammatory response to AgNP exposure. The inflammatory response was characterized by evaluating the production of the pro-inflammatory cytokines (A) TNF-α and (B) IL-6. * and † indicate statistical significance from untreated control and between static and dynamic conditions, respectively. n=3, $p<0.05$.

Implications of These Results

This work yielded a plethora of results that demonstrate how dynamic flow can impact the cellular response to AgNPs. First, this work showed the dependence of primary size and environmental factors in the cellular response to AgNPs. The results clearly showed how the 5 nm and 50 nm particles caused different responses from the cells. The 50 nm particles caused the cells to have a greater response with regards to viability, stress, and IL-6 secretion. These increased cellular responses correlated with the greater deposition of 50 nm particles over 5 nm.

In addition, this work determined that the static environment yielded a greater response with both AgNPs versus a dynamic environment. All the results from this work correlated back to AgNP deposition, which was dramatically decreased in the presence of dynamic flow. As NP deposition has been shown to dictate the extent of the cellular response, these results make sense. Each of the tests showed the greatest response for static 50 nm particles, which had the greatest deposition. Additionally, the results indicated an augmented difference in deposition between static and dynamic environments associated with 5 nm AgNPs, which correlates to the cellular data. Therefore this study reinforces the results for deposition and it highlights the importance of NP deposition on cellular response.

This work also emphasizes the impact of a dynamic environment on cellular behavior. Recreating a dynamic environment by using the peristaltic pump yielded different results than the static environment, for both the experimental AgNPs. As NPs are small, they are a likely target for dynamic movement as the forces induced by flow could significantly impact their mechanism of biotransport. The recreation of this environment was a necessary step to improve the accuracy in evaluating AgNPs behavior.

Most prominently, this study highlights how the addition of physiological factors can alter how cells interact with and respond to NPs. The dynamic environment much more accurately resembled the human body due to the movement, which arises in an in vivo system due to the presence of a cardiovascular system. Being able to create a more realistic in vitro model yields promise for more accurately understanding NP characterization and safety without the need for extensive animal testing.

Conclusion

The goal of the project was to identify how the presence of dynamic fluid movement impacts the deposition and cellular response to AgNPs of varying primary size. By using a peristaltic pump, a dynamic flow like the flow present in capillaries was created. This allowed for comparisons between static and dynamic environments for 5 and 50 nm AgNPs to be analyzed. Deposition dictated the cellular response of the A549 cells. The dynamic flow had the greatest effect on the smaller 5 nm particles due to their susceptibility to changes in biotransport. The 50 nm particles had the largest deposition, toxicity, cell stress, and immune response in static conditions due since they have the greatest mass and there was a lack of flow. This work is prominent due to the increased use of AgNPs within industry, which leads to increased human exposure such as through inhalation. Additionally, the ability to better simulate in vivo conditions by creating dynamic flow demonstrates how much of a difference cellular interactions and responses to AgNPs vary. Overall, this study helps to accurately understand how AgNPs behave within a physiologically similar environment.

Works Cited

1. Oldenburg, Steven J. "Silver nanoparticles: properties and applications." *Sigma–Aldrich.–2012* (2011).
2. Arora, Sumit, et al. "Silver nanoparticles protect human keratinocytes against UVB radiation-induced DNA damage and apoptosis: potential for prevention of skin carcinogenesis." *Nanomedicine: Nanotechnology, Biology and Medicine* 11.5 (2015): 1265-1275.
3. Palanki, Rohan, et al. "Size is an essential parameter in governing the UVB-protective efficacy of silver nanoparticles in human keratinocytes." *BMC cancer* 15.1 (2015): 636.
4. Chairuangkitti, Porntipa, et al. "Silver nanoparticles induce toxicity in A549 cells via ROS-dependent and ROS-independent pathways." *Toxicology in vitro* 27.1 (2013): 330-338.
5. Lu, Wentong, et al. "Effect of surface coating on the toxicity of silver nanomaterials on human skin keratinocytes." *Chemical physics letters* 487.1 (2010): 92-96.
6. Zanette, Caterina, et al. "Silver nanoparticles exert a long-lasting antiproliferative effect on human keratinocyte HaCaT cell line." *Toxicology in Vitro* 25.5 (2011): 1053-1060.
7. Comfort, Kristen K., et al. "Less is more: long-term in vitro exposure to low levels of silver nanoparticles provides new insights for nanomaterial evaluation." *ACS nano* 8.4 (2014).
8. Breitner, Emily K., Saber M. Hussain, and Kristen K. Comfort. "The role of biological fluid and dynamic flow in the behavior and cellular interactions of gold nanoparticles." *Journal of nanobiotechnology* 13.1 (2015): 56.